

# MR Prediction of Malignant Switch With the Cyst Fluid's T2 Value in Intraductal Papillary Mucinous Neoplasm of the Pancreas: A Preliminary Study

SEIICHIRO TAKAO<sup>1</sup>, AKIHIRO NISHIE<sup>1,2</sup>, YASUHIRO USHIJIMA<sup>1</sup>,  
YUKIHISA TAKAYAMA<sup>1</sup>, KOICHIRO MORITA<sup>1</sup>, KEISUKE ISHIMATSU<sup>1</sup>,  
YUTAKA KOGA<sup>3</sup>, YASUHISA MORI<sup>4</sup>, YUTA AKAMINE<sup>5</sup> and KOUSEI ISHIGAMI<sup>1</sup>

<sup>1</sup>Department of Clinical Radiology, Graduate School of Medical Sciences, Kyushu University, Fukuoka, Japan;

<sup>2</sup>Department of Radiology, Graduate School of Medical Science, University of the Ryukyus, Okinawa, Japan;

<sup>3</sup>Departments of Anatomic Pathology, Graduate School of Medical Sciences, Kyushu University, Fukuoka, Japan;

<sup>4</sup>Department of Surgery and Oncology, Graduate School of Medical Sciences, Kyushu University, Fukuoka, Japan;

<sup>5</sup>Philips Japan, Tokyo, Japan

**Abstract.** *Background/Aim:* We investigated whether the malignant switch of intraductal papillary mucinous neoplasm (IPMN) of the pancreas can be predicted by using the T1 $\rho$ , T2, and apparent diffusion coefficient (ADC) values of cyst fluid. *Patients and Methods:* We retrospectively analyzed the magnetic resonance (MR) images of 60 patients (26 males, 34 females, mean age 61 years) with branch-duct type and mixed-type IPMNs. The IPMNs were diagnosed clinically in 39 patients and histologically in 21 patients. The malignant potential was classified by MR imaging based on the international consensus guidelines for the management of IPMN established in 2017. Morphologically, 42 patients had "worrisome features" and three had "high-risk stigmata." Histologically, 14 lesions were diagnosed as low-grade dysplasia and seven as intermediate-grade dysplasia. The T1 $\rho$ , T2, and ADC values of cyst fluid in each patient's largest cyst were measured on the same slice, avoiding solid components. Spearman's rank correlation test was used to determine the correlation between the morphological malignancy and the T1 $\rho$ , T2, and ADC values. These values were also compared between the low-grade and intermediate-grade groups by Mann-Whitney U-test. *Results:* There was a significant rank-correlation between the morphological classification and T2 value ( $p=0.04$ ). The T2 value of the

intermediate-grade group was significantly higher than that of the low-grade group ( $p=0.03$ ). No significant correlations were morphologically or histologically obtained regarding T1 $\rho$  and ADC. *Conclusion:* The T2 value of cyst fluid together with other MR-signs may be useful for predicting the malignant switch in IPMN of the pancreas.

The identification of intraductal papillary mucinous neoplasms (IPMNs) is increasing with the improvements of diagnostic imaging. IPMNs exhibit a spectrum of neoplastic transformation and are not always carcinomas (1, 2), and thus patients with IPMNs may not necessarily need surgery or chemotherapy. However, some IPMNs evolve over time and can become malignant, and therefore surveillance is carried out for most patients with IPMNs (3). Important roles in this surveillance are held by imaging procedures such as computed tomography (CT), ultrasonography (US), and magnetic resonance imaging (MRI), because the malignancy of IPMNs is assessed based on morphological features including the size of the cysts, the diameter of the main pancreatic duct (MPD), and the presence of mural nodules (4, 5). The cyst fluid from IPMNs has not been a focus of assessment of IPMNs and their malignancy, but the aspects of cyst fluid such as the type of mucin, pH, tumor protein, and glucose concentration can vary according to the degree of malignancy (6-8).

Endoscopic ultrasound-fine needle aspiration (EUS-FNA) is one of the diagnostic methods used to evaluate cyst fluid, but it cannot be performed easily because it is an invasive procedure and may cause leakage of the cyst contents, potentially leading to peritoneal dissemination or gastric seeding (9, 10). A new noninvasive diagnostic method for determining the condition of cyst fluid is desired, as such a method could make the prediction of the malignant switch of IPMNs more accurate.

*Correspondence to:* Akihiro Nishie, MD, Ph.D., Department of Radiology, Graduate School of Medical Science, University of the Ryukyus, 207, Uehara, Nishihara-cho, Okinawa, 903-0215, Japan. Tel: +81 988951162, Fax: +81 988951420, e-mail: nishie\_a@med.u-ryukyu.ac.jp

**Key Words:** Pancreas, pancreatic intraductal neoplasms, multiparametric magnetic resonance imaging.

Table I. Morphological classification based on the International Consensus Guideline 2017.

Classification	Risk of malignancy	Findings
High-risk stigmata	Highly suggestive of malignancy	1) Obstructive jaundice in a patient with cystic lesion of the head of the pancreas 2) Enhancing mural nodule $\geq 5$ mm 3) MPD $\geq 10$ mm in size
Worrisome feature	Possible malignancy	1) Cyst $\geq 3$ cm 2) Enhancing mural nodule $< 5$ mm 3) Thickened/enhancing cyst walls 4) MPD size 5-9 mm 5) Abrupt change in caliber of pancreatic duct with distal pancreatic atrophy 6) Lymphadenopathy 7) Increased serum level of CA19-9 8) Cyst growth rate $\geq 5$ mm/2 years
Other	Not classified into HRS or WF	No WF and a definite branch duct type

HRS: High-risk stigmata; WF: worrisome features; OT: other; MPD: main pancreatic duct.

One of the existing noninvasive diagnostic methods for IPMNs is MRI, which is clinically used to evaluate internal properties of a lesion in addition to morphological features. Since patients with IPMNs require repeated imaging examinations for follow-up, MRI also has the advantage of avoiding repeated radiation exposures. The relaxation time characteristics such as T2 and T1 $\rho$  can be quantified with MRI. We speculated that these relaxation times as well as the apparent diffusion coefficient (ADC) measured on diffusion-weighted imaging (DWI) have the potential to describe the condition of cyst fluid. It was reported that these relaxation times are sensitive to changes in the macromolecular composition and the content of biological tissues (11). We hypothesized that if these parameters are indicative of the changes in cyst fluid, they could be a new biomarker for the assessment of the malignant switch of IPMNs. We conducted the present study to determine whether the malignant switch of IPMNs can be predicted by using the T1 $\rho$  value, T2 value, and/or ADC value of cyst fluid.

## Patients and Methods

**Patients.** This study was approved by the institutional review board of our hospital (approval no. 28-291). All methods were performed in accordance with the relevant guidelines and regulations, and all of the participants signed a written informed consent prior to their MRI scans.

Referring to the medical data recorded at our hospital, we retrospectively reviewed the MR images of 85 patients with branch-duct-type or mixed-type IPMNs examined during the 2.5-year period from October 2015 to April 2018. Patients were excluded for the following reasons: lack of scanning of T1 $\rho$ /T2 map (n=6), difficulty in evaluating the T2 map due to small cyst size (n=2), overlying artifacts (n=8), and a lesion outside of the scanning range (n=9). The final total of 60 patients were enrolled in the study. IPMNs were diagnosed clinically in 39 patients and histologically in the other 21 patients. There were 35 BD-IPMNs and 25 mixed-type IPMNs. The patients were 26 men and 34 women (age range=41-87 years; mean age 61 years).

**MR techniques.** All MRI scans were performed on a 3.0 T MRI scanner (Ingenia, Phillips Healthcare, Best, The Netherlands) with a 32-channel body coil. All 60 patients underwent MR examinations including magnetic resonance cholangiopancreatography (MRCP), T1 $\rho$  map, T2 map, and DWI. The imaging protocol included MRCP images [Repetition time (TR)/ Echo time (TE)=1,230/384 ms, echo train length=100, field of view (FOV)=30 $\times$ 30 cm; matrix=320 $\times$ 319, slice thickness=1 mm, volume thickness=80 mm, respiratory-triggered], DWI images (TR/TE=1,135/58 ms, FOV=38 $\times$ 38 cm; matrix=112 $\times$ 116, slice thickness=5 mm, intersection gap=1 mm, 0.676 half scan factor, 1 signal average, spectral pre-saturation inversion recovery, 2.5 SENSE factor, b-factor of 0, 500, and 1,000 s/mm<sup>2</sup>, diffusion gradients applied in three axes, 2.5 sections acquired. ADC maps were automatically generated on the operating console using all three images, with b-factors of 0, 500, and 1,000 s/mm<sup>2</sup>) and the T1 $\rho$ /T2 quantification sequence (TR/TE=1.6/5.4 ms, FOV=360 $\times$ 306 mm, matrix=160 $\times$ 128, slice thickness=10 mm, time of recovery=10,000 ms, number of slices=3; For T1 $\rho$ : the times of the spin lock pulse [TSL]=0/20/40/60 ms, spin-lock frequency=500 Hz; For T2: preparation TE=0/20/40/60ms; total acquisition time=17 s).

When a mural nodule was suspected on MRCP, fat-suppressed gradient-echo T1-weighted images with an enhanced three-dimensional T1 high-resolution isotropic volume excitation (eTHRIVE) were obtained before and after hand injection of a total amount of Gadobutrol (Gadovist: Bayer, Osaka, Japan) based on the patient's body weight (0.1 mmol/kg). The imaging parameters of eTHRIVE were as follows: TR/TE=3.0 ms/1.4 ms, flip angle (FA) 10°, matrix=252 $\times$ 200, FOV=36 $\times$ 36 cm, slice thickness/gap=3 mm/-1.5 mm, Spectral Selective Water Suppression Prepulse (SPAIR), scan time 17.9 s, and breath-holding.

### Image analysis.

**Evaluation of the malignant potential of IPMNs.** Morphological classification: We classified the IPMNs into three categories dependent on the interpretation results: "high-risk stigmata" (HRS), "worrisome feature" (WF), and "other" (OT). These malignancy categories were based on the International Consensus Guidelines 2017 for the management of IPMN and mucinous cystic neoplasm (MCN) of the pancreas (3) (Table I). Two radiologists (S.T. and A.N. with 7 and 23 years of experience as radiologists, respectively)

Table II. The correlation between morphological classification and cyst size, MPD, T1Q, T2 or ADC.

	Cyst size (mm)	MPD (mm)	T1Q (ms)	T2 (ms)	ADC ( $\times 10^{-3}$ mm <sup>2</sup> /s)
High-risk stigmata (n=3)	54 $\pm$ 29.2	11.7 $\pm$ 5.8	375.0 $\pm$ 68.8	423.4 $\pm$ 104.6	3.32 $\pm$ 0.58
Worrisome features (n=42)	38.4 $\pm$ 7.4	4.6 $\pm$ 2.0	361.2 $\pm$ 122.1	367.7 $\pm$ 109.7	3.12 $\pm$ 0.30
Other (n=15)	23.6 $\pm$ 4.5	3.4 $\pm$ 0.7	361.8 $\pm$ 135.7	307.5 $\pm$ 108.0	3.07 $\pm$ 0.26
Rho	0.69	0.40	-0.009	0.26	0.09
p-Value	<0.0001	0.0014	0.94	0.04	0.47

MPD: Main pancreatic duct; ADC: apparent diffusion coefficient.

Table III. Summary of cyst size, MPD diameter, T1Q value, T2 value or ADC value in histological classification.

	Cyst size (mm)	MPD (mm)	T1Q (ms)	T2 (ms)	ADC ( $\times 10^{-3}$ mm <sup>2</sup> /s)
Intermediate-grade dysplasia (n=7)	46.6 $\pm$ 19.4	6.0 $\pm$ 4.4	401.5 $\pm$ 68.9	406.9 $\pm$ 82.2	3.35 $\pm$ 0.32
Low-grade dysplasia (n=14)	33.9 $\pm$ 9.6	6.36 $\pm$ 3.7	331.1 $\pm$ 156.8	294.0 $\pm$ 112.5	3.10 $\pm$ 0.32
p-Value	0.08	0.40	0.40	0.03	0.14

MPD: Main pancreatic duct; ADC: apparent diffusion coefficient.

performed all the measurements of cyst size, the MPD dilatation, and the mural nodules on the MRCP images consensually using a picture archiving and communication system (PACS) workstation (Synapse; Fuji). They were blinded to the patients' histologic diagnosis as well as all clinical and laboratory information. Cyst size was defined as the major axis diameter on axial or coronal view. For multiple lesions, we mainly focused on the largest cyst. MPD diameter was recorded at the maximal point of MPD dilatation. Mural nodules were defined as hyperdense nodules that protruded into the dilated branch duct, which enhanced after the use of contrast agents during MRI.

*Measurement of the T1Q, T2, and ADC values of the IPMNs.* For the measurement of the T1Q and T2 values, the T1Q and T2 maps were generated by using original software in an Interface Definition Language (IDL) virtual machine. T1Q and T2 maps were reconstructed by fitting the T1Q- and T2-weighted images voxel-by-voxel to the following equations:

$$\text{T1Q map: } S(TSL) = S(0) \times \exp(-TSL/T1Q)$$

$$\text{T2 map: } S(TE) = S(0) \times \exp(-TE/T2)$$

The T1Q and T2 values were measured by using the software ImageJ (ver. 1.80, U.S. National Institutes of Health, MA, USA). We selected a slice on each cyst that appeared to be the largest of the three slices and then placed as large a region-of-interest (ROI) as possible on the T1Q and T2 maps, avoiding areas of artifacts and solid parts.

We measured the ADC values by using a PACS workstation. We selected the same slice on which the T1Q and T2 values were measured and then placed as large an ROI as possible on the ADC map, avoiding areas of artifacts and solid parts.

*Histological analysis.* Twenty-one IPMNs confirmed by surgery (n=1) or biopsy (n=20) were assessed by one pathologist (Y.K., with 10 years of experience as a pathologist). The lesions were

subcategorized based on the degree of dysplasia, consistent with the 2010 World Health Organization classification. The most predominant degree of dysplasia was recorded for each lesion.

*Statistical analysis.* We assessed the correlations between the morphological classification (*i.e.*, HRS, WF, OT) and the MRI findings such as cyst size, MPD diameter, T1Q value, T2 value, and ADC value by using Spearman's rank correlation test. The comparison of the average cyst size, MPD diameter, T1Q value, T2 value, or ADC value with the histological classification was performed using the Mann-Whitney *U*-test. Results with *p*-values <0.05 were considered significant. All analyses were performed using R ver. 3.1.1 software (12).

## Results

*Morphological and histological classification findings.* By the morphological examination, the 60 patients were classified into HRS (n=3), WF (n=42), and OT (n=15). The 21 histologically confirmed IPMNs were classified into seven cases with intermediate-grade dysplasia and 14 cases with low-grade dysplasia.

*Correlations between the morphological classifications and MRI findings.* Table II shows the correlations between the morphological classifications and the cyst size, MPD diameter, T1Q value, T2 value, or ADC value. In addition to cyst size and MPD diameter, the T2 value was also significantly associated with the morphological malignancy (Figure 1). In contrast, there was no significant rank-correlation between the morphological classification and the T1Q value or the ADC value (Figure 2).

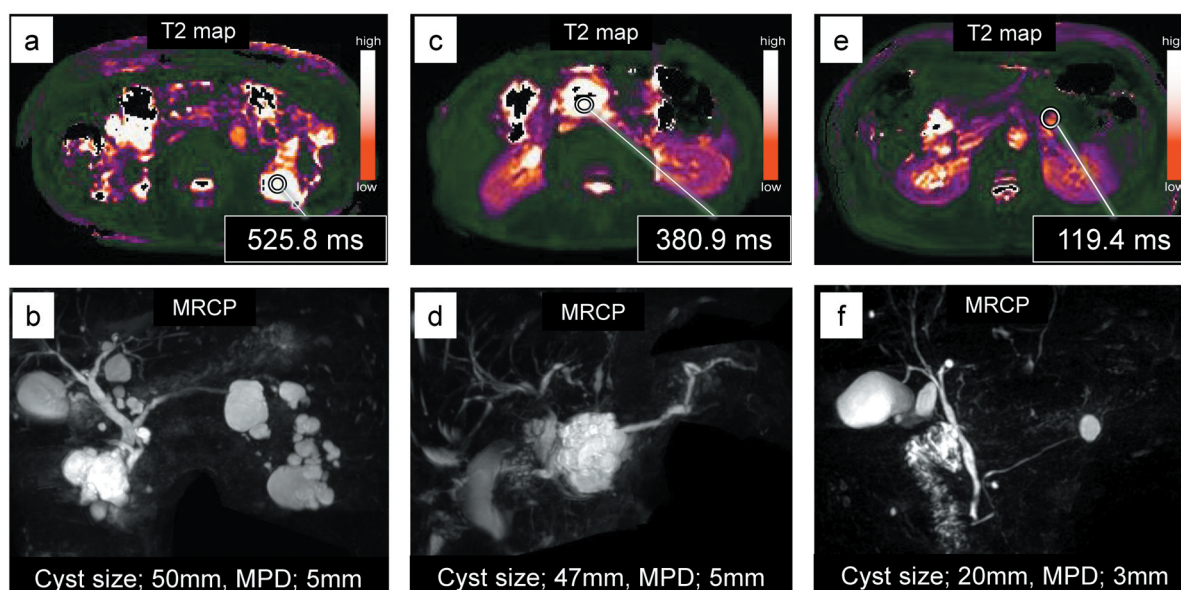


Figure 1. Clinical cases' T2 map and MRCP findings in high-risk stigmata (HRS), worrisome feature (WF), and other (OT). A, B) Representative HRS case with an enhancing solid component within the cyst. A) A high T2 value (525.8 ms) was shown on the T2 map. B) Magnetic resonance cholangiopancreatography (MRCP) findings: Intraductal papillary mucinous neoplasm of the secondary duct, multifocal (located in the head, body and tail). C, D) Representative WF case due to cyst size. C) A moderate T2 value (380.9 ms) was shown on the T2 map. D) MRCP: Intraductal papillary mucinous neoplasm of the secondary duct, located in the head. E, F) Representative OT case. E) A low T2 value (119.4 ms) was shown on the T2 map. F) MRCP: Intraductal papillary mucinous neoplasm of the secondary duct, located in the tail.

**Comparison of MRI findings with the histological classifications.** Table III compares the MRI findings between the intermediate-grade dysplasia group (n=7) and the low-grade dysplasia group (n=14). The T2 values were significantly higher in the intermediate-grade dysplasia group compared to those in the low-grade dysplasia group (Figure 3). There was no significant difference between the two groups in cyst size, MPD diameter, T1 $\rho$  value or ADC value (Figure 4).

## Discussion

The results of our present retrospective analysis demonstrated that 1) there was a significant rank-correlation between the morphological classification and the T2 values of cyst fluid, and 2) the T2 values of the intermediate-grade dysplasia group were significantly higher than those of the low-grade dysplasia group. To our knowledge, this is the first study to demonstrate a relationship between the T2 value and the degree of malignancy in IPMN. The histology reflects the malignancy of a target IPMN, while the morphology of the malignancy reflects both the target lesion and its progress. However, cyst fluid's T2 values were correlated with two kinds of malignancy set up in the present study.

Radiological modalities such as CT and MRI play a vital role in the surveillance of IPMNs, but the existing literature regarding their diagnostic accuracy and ability to assess the

involvement and size of the main pancreatic duct in IPMN is limited (13, 14). According to the International Consensus Guidelines 20173, EUS is recommended when worrisome features are suspected on CT/MRI. In addition, MRI has shown less accurate results than EUS to identify nodules and/or vegetation (15). These findings represent the limitations of MRI for surveillance. In contrast, recent studies used cystic fluid not only for diagnosis but also to assess the tumor grade (16-18). Therefore, the assessment of cyst fluid could improve the management of IPMNs using MRI.

Our present findings revealed that of the T2, T1 $\rho$ , and ADC values, only the T2 value can be associated with the degree of malignancy in IPMN. One of the causes of this result is the mucin profile. Mucin is a hydrophilic macromolecular substance. In earlier research, core proteins for mucins (MUCs) were detected by immunohistochemistry. The mucin expression profile of IPMN cells is a major contributor to the phenotypic classification of IPMNs and is associated with the degree of malignancy. It was shown that IPMNs with an aggressive behavior and a poor outcome expressed MUC1 but did not express MUC2, whereas IPMNs with indolent behavior and a favorable outcome did not express MUC1 but did express MUC2 (19-23). MUC1 is one of the membrane-tethered mucins expressed on the surface of epithelial cells. In contrast, MUC2 is one of the human gel-forming secreted mucins.

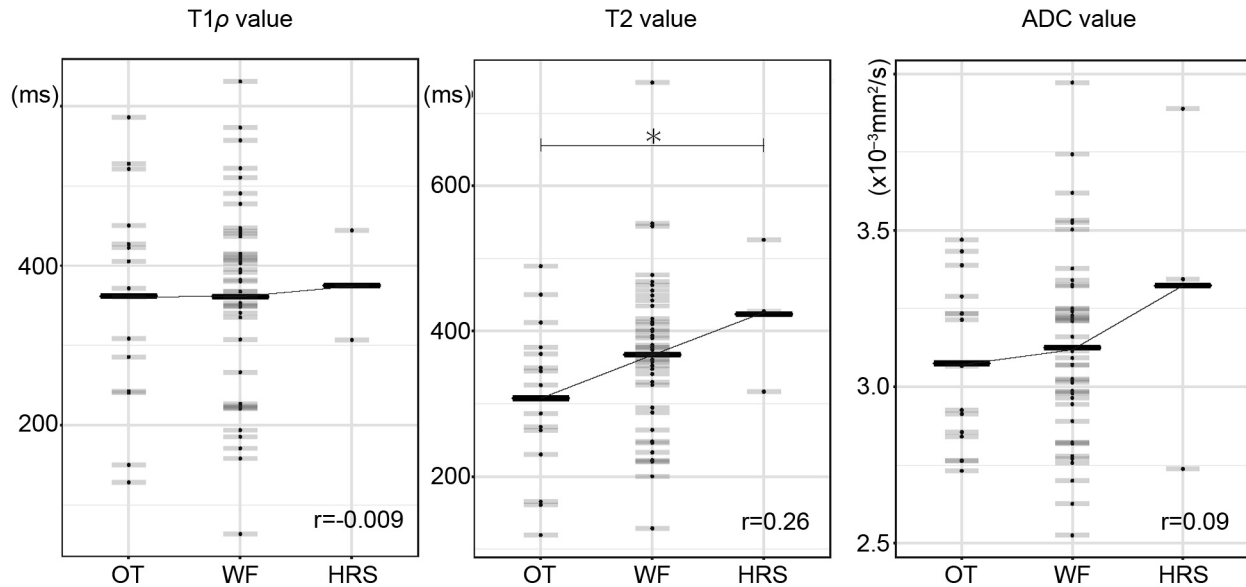


Figure 2. Rank-correlations between the morphological classification and the T1 $\rho$  value, T2 value, or ADC value. The T2 value was significantly associated with the morphological classification ( $p=0.04$ ,  $r=0.26$ ).  $*p<0.05$ , OT: other, WF: worrisome features, HRS: high-risk stigmata.

We hypothesize that the binding of water to mucin results in an increase in the amount of bound water, a decrease in the tumbling rate of protons, and finally the occurrence of the T2 shortening effect. Because T2 values were measured by placing ROIs in the center of IPMNs, the T2 values should be lower in MUC2-positive cysts (which are suggestive of less malignancy) and higher in MUC1-positive cysts (suggestive of more malignancy). This hypothesis can account for the present observation that the T2 value was higher in both the morphologically and histologically malignant groups. Considering that IPMNs exhibit a spectrum of neoplastic transformation, using the T2 value may predict malignant switch of IPMNs earlier than doing so based on the morphological transformation.

In fact, we observed that the cyst size and MPD diameter did not differ significantly between our patients with intermediate-grade dysplasia and those with low-grade dysplasia. The T2 value of the cyst fluid may enhance the diagnostic performance of the malignant potential and may be useful for the management of IPMN. For instance, in cases in which the T2 value of the cyst becomes higher during surveillance, it might be better to shorten the follow-up interval or to perform another work-up for the IPMN in order to capture malignant transformation earlier.

New imaging techniques such as the T1 $\rho$  map reveal the molecular level and could provide new perspectives in the imaging of IPMN. The cyst fluid of an IPMN changes as its malignancy progresses. The T1 $\rho$  value of the IPMN can be

used to investigate tumor components by reflecting the interactions between motion-restricted water molecules and their local macromolecular environment. However, our present analyses revealed no correlation between the T1 $\rho$  values and the degree of malignancy of the IPMNs. There were several reasons for this result, as follows. First, the optimal scan settings remain obscure because there are no previous studies of T1 $\rho$  maps for IPMNs. The TSL and TE used herein were set at values related to previous investigations on the prediction of liver fibrosis (24, 25). Second, the T1 $\rho$  value could be too long to be measured due to the noise, because a long TSL provides low signal intensity. Third, a quantitative evaluation of cyst fluid using T1 $\rho$  mapping may not be appropriate for predicting the malignancy of IPMNs because the water molecule dispersion within the cyst is too large. The development of a new scanning technique may enhance the performance of T1 $\rho$  mapping. This is an important issue to be solved in future research.

Our analyses also showed that there was no significant difference in the ADC values between the present low-grade dysplasia and intermediate-grade dysplasia groups. In earlier studies, benign lesions tended to have lower cyst fluid viscosity than more malignant lesions (26, 27), which may indicate that the diffusion in low-grade IPMNs is less restricted. In fact, several research groups have described the utility of ADC values for assessing the aggressiveness of IPMNs (28-31). Those researchers reported lower ADC values in branch-duct IPMNs with high-grade dysplasia (28), in malignant IPMNs

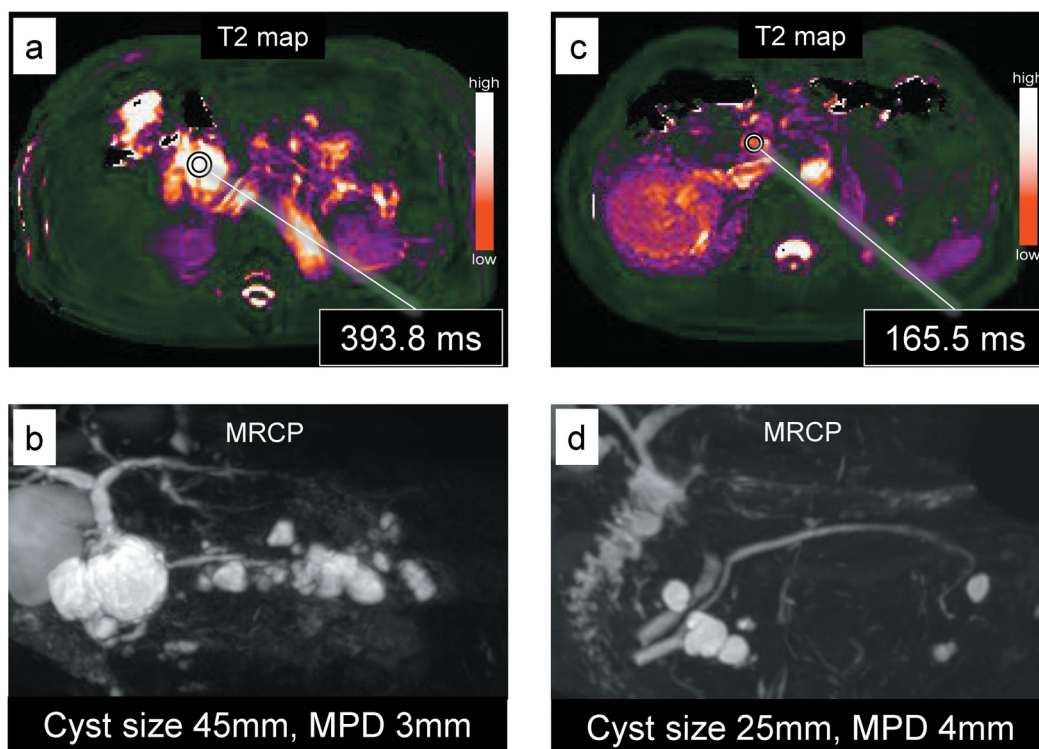


Figure 3. Clinical cases' T2 map and magnetic resonance cholangiopancreatography (MRCP) in intermediate-grade dysplasia and low-grade dysplasia. A, B) Representative case of intermediate-grade dysplasia IPMN. A) A high T2 value (393.8 ms) was shown on the T2 map. B) MRCP: Intraductal papillary mucinous neoplasm of the secondary duct, multifocal (located in the head, body and tail). C, D) Representative case of low-grade dysplasia IPMN. C) A low T2 value (165.5 ms) was shown on the T2 map. D) MRCP: Intraductal papillary mucinous neoplasm of the secondary duct, multifocal (located in the head and tail).

(30), and in IPMNs with a focal invasive component (31). These studies defined low-grade dysplasia or intermediate-grade dysplasia as benign IPMN. Our present findings are thus consistent with those of the previous reports. Simply put, an ADC map may be inappropriate for predicting the malignancy of incipient IPMNs.

In recent years, detailed histologic and genetic analyses have clarified the mechanisms underlying the progression from IPMN to pancreatic ductal adenocarcinoma (PDAC) (32). There are three different pathways of progression: the sequential subtype, the branch-off subtype, and the de novo subtype. The field carcinogenesis of each of these pathways differs, and the precursors – including incipient IPMN – are already diverse (32). The characteristics of incipient IPMNs could thus be important for surveillance; that is, our results suggest that only T2 mapping may be useful for the detection of malignant switch of IPMNs at the stage of early neoplastic change.

This study has some limitations. There could have been an influence of the partial volume effect on the measurement of the T1 $\rho$  and/or T2 values, especially for small-sized lesions. However, there was no significant difference in lesion size

between our low-grade and intermediate-grade dysplasia groups. There could also have been differences in the slice level between the images obtained with different TSL or TE values. Our cohort had a small number of IPMNs classified as HRS (n=3) and no IPMN classified as being in the high-grade dysplasia group. Thus, to translate T2 imaging into clinical applications for use as an early imaging biomarker of the IPMN grade, further technical improvements and larger HRS cohorts are warranted. In addition, the histological confirmation of IPMN was obtained by biopsy, not surgery. The most predominant degree of dysplasia may be actually changed. Finally, this study focused on cyst fluid and did not assess the risk of the entire pancreas, such as PDAC concomitant with IPMN. However, it seems appropriate to focus on cyst fluid of incipient IPMNs from the standpoint of their progression to PDAC because the incipient IPMNs are already diverse.

In conclusion, the T2 value of cyst fluid was significantly increased as the malignancy of IPMNs advanced morphologically and histologically. The T2 value of cyst fluid may be useful for predicting the malignant switch in IPMN of the pancreas.

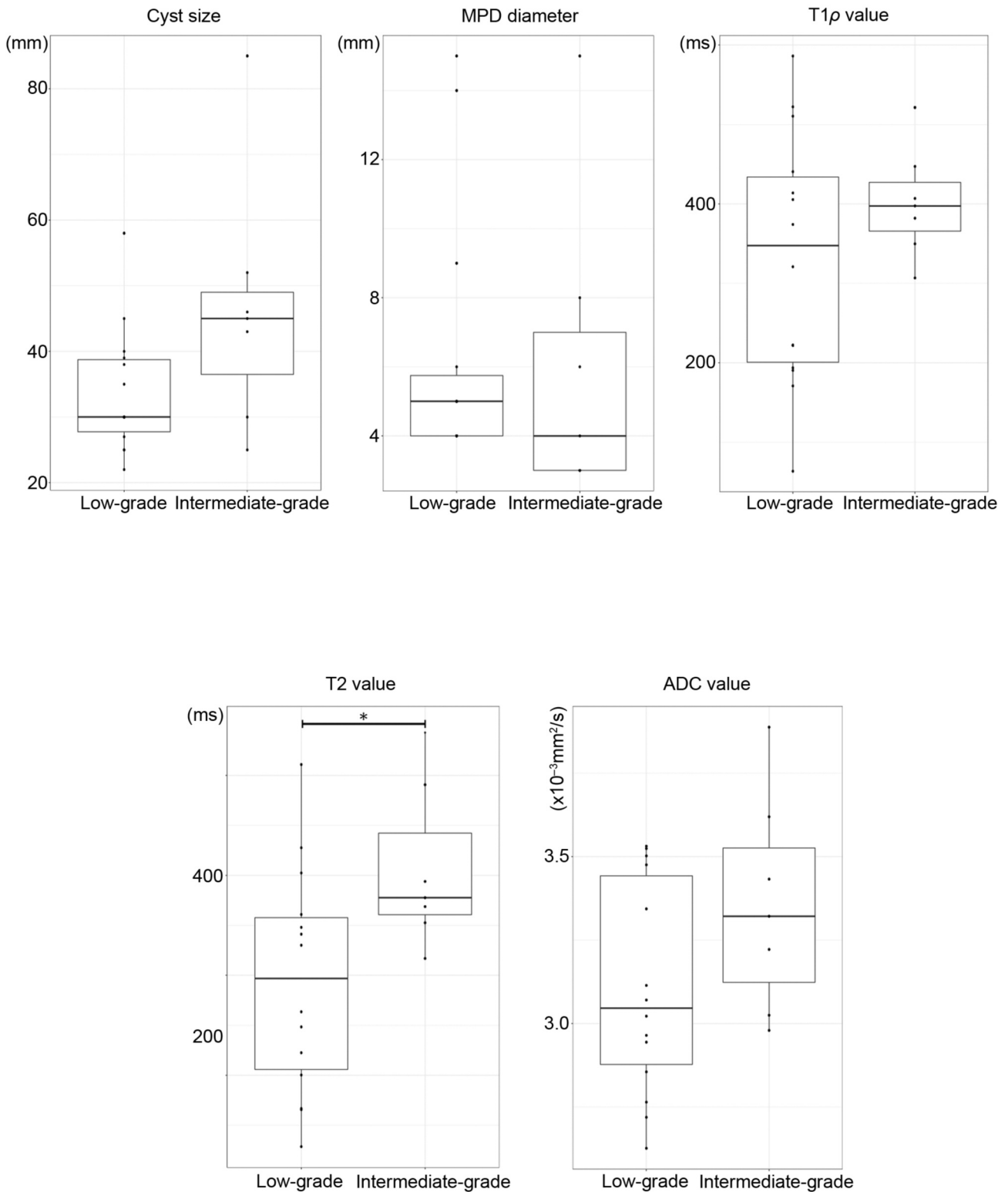


Figure 4. Box plot showed comparisons between low-grade dysplasia (low-grade) and intermediate-grade dysplasia (intermediate-grade) in each parameter: cyst size, main pancreatic duct (MPD) diameter, T1ρ value, T2 value, and apparent diffusion coefficient (ADC) value. The box shows the interquartile range (IQR). The whiskers add 1.5 times the IQR to the 75<sup>th</sup> percentile and subtract 1.5 times the IQR from the 25<sup>th</sup> percentile. The T2 value was significantly higher in the intermediated-grade dysplasia group than in the low-grade dysplasia ( $p=0.03$ ).

## Conflicts of Interest

Yuta Akamine is an employee of Philips Healthcare, but not implicated in any data analysis. Seiichiro Takao, Akihiro Nishie, Yasuhiro Ushijima, Yukihisa Takayama, Koichiro Morita, Keisuke Ishimatsu, Yutaka Koga, Yasuhisa Mori and Kousei Ishigami have no relevant conflicts of interest to disclose.

## Authors' Contributions

All the Authors have contributed significantly to the concept design of this manuscript, and the work leading to the final manuscript. All Authors have reviewed the article and agreed to its content.

## Acknowledgements

The Authors thank Prof. Masafumi Nakamura, Department of Surgery and Oncology, Kyushu University, for providing clinical information for this manuscript. This work was supported by a Grant-in-Aid for Scientific Research (C), JSPS KAKENHI grant no. 17K10409. The Authors also thank Prof. Yoshinao Oda, Department of Anatomic Pathology, Kyushu University, for providing the pathological information for this manuscript.

## References

- 1 Adsay NV, Fukushima N, Furukawa T, Hruban RH and Klimstra DS: Intraductal neoplasms of the pancreas. *In: Bosman FT, Carneiro F, Hruban RH, Theise ND, editors. WHO Classification of Tumours of the Digestive System. Lyon: IARC, 2010, pp. 304-313.*
- 2 Hruban RH, Pitman MB and Klimstra DS: Intraductal Neoplasms AFIP Atlas of Tumor Pathology. *In: Tumors of the Pancreas Vol. 6., Washington DC: American Registry of Pathology, 2007, pp. 75-110.*
- 3 Tanaka M, Fernández-Del Castillo C, Kamisawa T, Jang JY, Levy P, Ohtsuka T, Salvia R, Shimizu Y, Tada M and Wolfgang CL: Revisions of international consensus Fukuoka guidelines for the management of IPMN of the pancreas. *Pancreatology 17(5): 738-753, 2017. PMID: 28735806. DOI: 10.1016/j.pan.2017.07.007*
- 4 Marchegiani G, Andrianello S, Borin A, Dal Borgo C, Perri G, Pollini T, Romanò G, D'Onofrio M, Gabbriellini A, Scarpa A, Malleo G, Bassi C and Salvia R: Systematic review, meta-analysis, and a high-volume center experience supporting the new role of mural nodules proposed by the updated 2017 international guidelines on IPMN of the pancreas. *Surgery 163(6): 1272-1279, 2018. PMID: 29454468. DOI: 10.1016/j.surg.2018.01.009*
- 5 Hwang DW, Jang JY, Lee SE, Lim CS, Lee KU and Kim SW: Clinicopathologic analysis of surgically proven intraductal papillary mucinous neoplasms of the pancreas in SNUH: a 15-year experience at a single academic institution. *Langenbecks Arch Surg 397(1): 93-102, 2012. PMID: 20640860. DOI: 10.1007/s00423-010-0674-6*
- 6 Wang W, Zhang L, Chen L, Wei J, Sun Q, Xie Q, Zhou X, Zhou D, Huang P, Yang Q, Xie H, Zhou L and Zheng S: Serum carcinoembryonic antigen and carbohydrate antigen 19-9 for prediction of malignancy and invasiveness in intraductal papillary mucinous neoplasms of the pancreas: A meta-analysis. *Biomed Rep 3(1): 43-50, 2015. PMID: 25469245. DOI: 10.3892/br.2014.376*
- 7 Hibi Y, Fukushima N, Tsuchida A, Sofuni A, Itoi T, Moriyasu F, Mukai K and Aoki T: Pancreatic juice cytology and subclassification of intraductal papillary mucinous neoplasms of the pancreas. *Pancreas 34(2): 197-204, 2007. PMID: 17312458. DOI: 10.1097/MPA.0b013e31802dea0*
- 8 Moris D, Damaskos C, Spartalis E, Papalampros A, Vernadakis S, Dimitroulis D, Griniatsos J, Felekouras E and Nikiteas N: Updates and critical evaluation on novel biomarkers for the malignant progression of intraductal papillary mucinous neoplasms of the pancreas. *Anticancer Res 37(5): 2185-2194, 2017. PMID: 28476781. DOI: 10.21873/anticancer.11553*
- 9 Hirooka Y, Goto H, Itoh A, Hashimoto S, Niwa K, Ishikawa H, Okada N, Itoh T and Kawashima H: Case of intraductal papillary mucinous tumor in which endosonography-guided fine-needle aspiration biopsy caused dissemination. *J Gastroenterol Hepatol 18(11): 1323-1324, 2003. PMID: 14535994. DOI: 10.1046/j.1440-1746.2003.03040.x*
- 10 Ahmed K, Sussman JJ, Wang J and Schmulewitz N: A case of EUS-guided FNA-related pancreatic cancer metastasis to the stomach. *Gastrointest Endosc 74(1): 231-233, 2011. PMID: 21168837. DOI: 10.1016/j.gie.2010.10.008*
- 11 Wang YX, Yuan J, Chu ES, Go MY, Huang H, Ahuja AT, Sung JJ and Yu J: T1rho MR imaging is sensitive to evaluate liver fibrosis: an experimental study in a rat biliary duct ligation model. *Radiology 259(3): 712-719, 2011. PMID: 21436087. DOI: 10.1148/radiol.11101638*
- 12 <http://www.R-project.org/>
- 13 Kang HJ, Lee JM, Joo I, Hur BY, Jeon JH, Jang JY, Lee K, Ryu JK, Han JK and Choi BI: Assessment of malignant potential in intraductal papillary mucinous neoplasms of the pancreas: Comparison between multidetector CT and MR imaging with MR cholangiopancreatography. *Radiology 279(1): 128-139, 2016. PMID: 26517448. DOI: 10.1148/radiol.2015150217*
- 14 Sahani D, Prasad S, Saini S and Mueller P: Cystic pancreatic neoplasms evaluation by CT and magnetic resonance cholangiopancreatography. *Gastrointest Endosc Clin N Am 12(4): 657-672, 2002. PMID: 12607778. DOI: 10.1016/s1052-5157(02)00022-3*
- 15 Costa DAPD, Guerra JG, Goldman SM, Kemp R, Santos JS, Ardengh JC, Ribas CAPM, Nassif PAN and Ribas-Filho JM: Magnetic resonance cholangiopancreatography (MRCP) versus endosonography-guided fine needle aspiration (EUS-FNA) for diagnosis and follow-up of pancreatic intraductal papillary mucinous neoplasms. *Arq Bras Cir Dig 32(4): e1471, 2019. PMID: 31859924. DOI: 10.1590/0102-672020190001e1471*
- 16 Faias S, Pereira L, Roque R, Chaves P, Torres J, Cravo M and Pereira AD: Excellent accuracy of glucose level in cystic fluid for diagnosis of pancreatic mucinous cysts. *Dig Dis Sci 65(7): 2071-2078, 2020. PMID: 31705344. DOI: 10.1007/s10620-019-05936-5*
- 17 Levy A, Popovici T and Bories PN: Tumor markers in pancreatic cystic fluids for diagnosis of malignant cysts. *Int J Biol Markers 32(3): e291-e296, 2017. PMID: 28315508. DOI: 10.5301/ijbm.5000257*
- 18 Al Efishat MA, Attiyeh MA, Eaton AA, Gönen M, Prosser D, Lokshin AE, Castillo CF, Lillemoe KD, Ferrone CR, Pergolini I, Mino-Kenudson M, Rezaee N, Dal Molin M, Weiss MJ, Cameron JL, Hruban RH, D'Angelica MI, Kingham TP, DeMatteo RP, Jarnagin WR, Wolfgang CL and Allen PJ: Multi-institutional validation study of pancreatic cyst fluid protein

- analysis for prediction of high-risk intraductal papillary mucinous neoplasms of the pancreas. *Ann Surg* 268(2): 340-347, 2018. PMID: 28700444. DOI: 10.1097/SLA.0000000000002421
- 19 Osako M, Yonezawa S, Siddiki B, Huang J, Ho JJ, Kim YS and Sato E: Immunohistochemical study of mucin carbohydrates and core proteins in human pancreatic tumors. *Cancer* 71(7): 2191-2199, 1993. PMID: 8384065. DOI: 10.1002/1097-0142(19930401)71:7<2191::aid-cnrcr2820710705>3.0.co;2-x
- 20 Osako M, Yonezawa S, Yamashita K, Shimizu T, Tanaka S, Mizouchi J, Tabata M, Sakamoto H, Sato E and Sakoda K: Immunohistochemical studies of mucin antigens in pancreas and intrahepatic bile-duct tumors. *Journal of Hepato-Biliary-Pancreatic Surgery* 4(2): 149-156, 2021. DOI: 10.1007/BF02489780
- 21 Yonezawa S, Higashi M, Yamada N, Yokoyama S and Goto M: Significance of mucin expression in pancreatobiliary neoplasms. *J Hepatobiliary Pancreat Sci* 17(2): 108-124, 2010. PMID: 19787286. DOI: 10.1007/s00534-009-0174-7
- 22 Hollingsworth MA and Swanson BJ: Mucins in cancer: protection and control of the cell surface. *Nat Rev Cancer* 4(1): 45-60, 2004. PMID: 14681689. DOI: 10.1038/nrc1251
- 23 Castellano-Megías VM, Andrés CI, López-Alonso G and Colina-Ruizdelgado F: Pathological features and diagnosis of intraductal papillary mucinous neoplasm of the pancreas. *World J Gastrointest Oncol* 6(9): 311-324, 2014. PMID: 25232456. DOI: 10.4251/wjgo.v6.i9.311
- 24 Okuaki T, Takayama Y, Nishie A, Ogino T, Obara M, Honda H, Miyati T and Van Cauteren M: T<sub>1</sub>ρ mapping improvement using stretched-type adiabatic locking pulses for assessment of human liver function at 3T. *Magn Reson Imaging* 40: 17-23, 2017. PMID: 28363761. DOI: 10.1016/j.mri.2017.03.006
- 25 Li X, Wyatt C, Rivoire J, Han E, Chen W, Schooler J, Liang F, Shet K, Souza R and Majumdar S: Simultaneous acquisition of T1ρ and T2 quantification in knee cartilage: repeatability and diurnal variation. *J Magn Reson Imaging* 39(5): 1287-1293, 2014. PMID: 23897756. DOI: 10.1002/jmri.24253
- 26 Linder JD, Geenen JE and Catalano MF: Cyst fluid analysis obtained by EUS-guided FNA in the evaluation of discrete cystic neoplasms of the pancreas: a prospective single-center experience. *Gastrointest Endosc* 64(5): 697-702, 2006. PMID: 17055859. DOI: 10.1016/j.gie.2006.01.070
- 27 Leung KK, Ross WA, Evans D, Fleming J, Lin E, Tamm EP and Lee JH: Pancreatic cystic neoplasm: the role of cyst morphology, cyst fluid analysis, and expectant management. *Ann Surg Oncol* 16(10): 2818-2824, 2009. PMID: 19536601. DOI: 10.1245/s10434-009-0502-9
- 28 Sandrasegaran K, Akisik FM, Patel AA, Rydberg M, Cramer HM, Agaram NP and Schmidt CM: Diffusion-weighted imaging in characterization of cystic pancreatic lesions. *Clin Radiol* 66(9): 808-814, 2011. PMID: 21601184. DOI: 10.1016/j.crad.2011.01.016
- 29 Hoffman DH, Ream JM, Hajdu CH and Rosenkrantz AB: Utility of whole-lesion ADC histogram metrics for assessing the malignant potential of pancreatic intraductal papillary mucinous neoplasms (IPMNs). *Abdom Radiol (NY)* 42(4): 1222-1228, 2017. PMID: 27900458. DOI: 10.1007/s00261-016-1001-7
- 30 Kang KM, Lee JM, Shin CI, Baek JH, Kim SH, Yoon JH, Han JK and Choi BI: Added value of diffusion-weighted imaging to MR cholangiopancreatography with unenhanced mr imaging for predicting malignancy or invasiveness of intraductal papillary mucinous neoplasm of the pancreas. *J Magn Reson Imaging* 38(3): 555-563, 2013. PMID: 23390008. DOI: 10.1002/jmri.24022
- 31 Ogawa T, Horaguchi J, Fujita N, Noda Y, Kobayashi G, Ito K, Koshita S, Kanno Y, Masu K and Sugita R: Diffusion-weighted magnetic resonance imaging for evaluating the histological degree of malignancy in patients with intraductal papillary mucinous neoplasm. *J Hepatobiliary Pancreat Sci* 21(11): 801-808, 2014. PMID: 25082473. DOI: 10.1002/jhbp.135
- 32 Omori Y, Ono Y, Tanino M, Karasaki H, Yamaguchi H, Furukawa T, Enomoto K, Ueda J, Sumi A, Katayama J, Muraki M, Taniue K, Takahashi K, Ambo Y, Shinohara T, Nishihara H, Sasajima J, Maguchi H, Mizukami Y, Okumura T and Tanaka S: Pathways of progression from intraductal papillary mucinous neoplasm to pancreatic ductal adenocarcinoma based on molecular features. *Gastroenterology* 156(3): 647-661.e2, 2019. PMID: 30342036. DOI: 10.1053/j.gastro.2018.10.029

Received June 1, 2022

Revised June 24, 2022

Accepted June 24, 2022